Journal Pre-proof

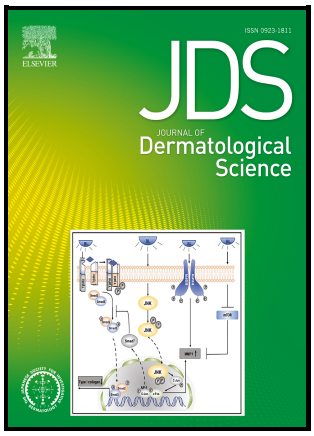

CHARACTERISATION OF SUPERFICIAL CORNEOCYTE PROPERTIES OVER CATEGORY I PRESSURE ULCERS: INSIGHTS INTO TOPOGRAPHICAL AND MATURATION CHANGES

Ana S. Évora, Nkemjika Abiakam, Zhibing Zhang, Simon A. Johnson, Michael J. Adams, Dan L. Bader, Peter R. Worsley

PII: S0923-1811(23)00185-8

DOI: https://doi.org/10.1016/j.jdermsci.2023.08.008

Reference: DESC3951

To appear in: *Journal of Dermatological Science*

Received date: 31 May 2023
Revised date: 19 August 2023
Accepted date: 31 August 2023

Please cite this article as: Ana S. Évora, Nkemjika Abiakam, Zhibing Zhang, Simon A. Johnson, Michael J. Adams, Dan L. Bader and Peter R. Worsley, CHARACTERISATION OF SUPERFICIAL CORNEOCYTE PROPERTIES OVER CATEGORY I PRESSURE ULCERS: INSIGHTS INTO TOPOGRAPHICAL AND MATURATION CHANGES, *Journal of Dermatological Science,* (2023) doi:https://doi.org/10.1016/j.jdermsci.2023.08.008

CHARACTERISATION OF SUPERFICIAL CORNEOCYTE PROPERTIES OVER CATEGORY I PRESSURE ULCERS: INSIGHTS INTO TOPOGRAPHICAL AND MATURATION CHANGES

Ana S. Évora*[1], A.S.M.M.Evora@bham.ac.uk, ORCID: 0000-0003-1562-6105

Nkemjika Abiakam[2], N.S.Abiakam@soton.ac.uk, ORCID: 0000-0002-9599-7274

Zhibing Zhang[1], z.zhang@bham.ac.uk, ORCID: 0000-0003-2797-9098

Simon A. Johnson[1], s.a.johnson@bham.ac.uk, ORCID: 0000-0001-6621-7622

Michael J. Adams[1], m.j.adams@bham.ac.uk, ORCID: 0000-0001-9648-7308

Dan L. Bader[2], ORCID: 0000-0002-1208-3507

Peter R. Worsley[2], p.r.worsley@soton.ac.uk, ORCID: 0000-0003-0145-5042

[1]School of Chemical Engineering, University of Birmingham, Birmingham, UK

[2]School of Health Sciences, University of Southampton, Southampton, UK

***Corresponding author:** Ana S. Évora

Address: School of Chemical Engineering, University of Birmingham, UK

Email: A.S.M.M.Evora@bham.ac.uk

Funding source: This work was supported by the European Union's Horizon 2020 research and innovation programme under the Marie Skłodowska-Curie grant agreement No. 811965 (Project STINTS - Skin Tissue Integrity under Shear).

Conflict of Interest: The authors have no conflict of interest to declare.

Word count: 3461; **Figures:** 5; **Tables:** 1; **References:** 33

ABSTRACT

Background: Pressure ulcers (PUs) are chronic wounds that are detrimental to the quality of life of patients. Despite advances in monitoring skin changes, the structure and function of skin cells over the site of pressure ulcers are not fully understood.

Objective: The present study aims to evaluate local changes in the properties of superficial corneocytes in category 1 PU sites sampled from a cohort of hospitalised patients.

Methods: Cells were collected from a PU-compromised site and an adjacent control area and their topographical, maturation and mechanical properties were analysed.

Results: Corneocytes at the PU-compromised site were characterised by higher levels of immature cornified envelopes ($p<0.001$) and greater amounts of desmoglein-1 (corneodesmosomal protein) ($p<0.001$) compared to the adjacent control area. The cells at the control site presented the typical ridges-and-valleys

topographical features of sacrum corneocytes. By contrast, the PU cells presented circular nano-objects at the cell surface, and, for some patients, the cell topography was deformed. CEs at the PU site were also smaller than at the control site. Although differences were not observed in the mechanical properties of the cells, those of the elderly patients were much softer compared with young subjects.

Conclusion: This is the first study investigating the changes in corneocyte properties in category I pressure ulcers. Superficial cells at the PU sites showed altered topographical and maturation characteristics. Further studies are required to elucidate if these changes are a consequence of early loss of skin integrity or a result of mechanical and microclimate insults to the skin surface.

Keywords:

corneocytes, pressure ulcers, stratum corneum, desmoglein-1, cornified, envelope, atomic force microscopy

Abbreviations: Pressure ulcer, PU; Atomic force microscopy, AFM; Stratum corneum, SC; Cornified envelope, CE; Desmoglein-1, Dsg1; Corneodesmosome, CD; Circular nano-objects, CNOs; Transepidermal water loss, TEWL.

INTRODUCTION

A pressure ulcer (PU) has been defined as localised damage to the skin and/or underlying tissue, as a result of pressure alone or in combination with shear, usually occurring over a bony prominence and may also be related to the application of a medical device or other objects [1, 2]. However, as suggested by late Emeritus Professor Dan Bader in his recent editorial “The last hurrah”, there has been a recent overemphasis on deep tissue injury (DTI) in the literature [3, 4]. This ignores the fact that most PUs are classified as category I and II and are initiated at the superficial dermal and epidermal layers, with interactions of pressure, shear, friction and moisture [5]. Although the role of the dermis on the architecture and mechanical function of the skin has been studied [6, 7], the potential role of the epidermis, and particularly that of the Stratum Corneum (SC), is usually neglected.

The SC can be considered a thin stiff film of dead cells on top of softer viable tissues [8-10]. At low relative humidities (RH ~30–40%), the SC acts as a polymer in a glassy state, with Young’s moduli values of the order of GPa [8], i.e., a factor of 10^5 greater than that of the dermis [11]. As a result of the characteristic mechanical properties, the role of the SC, and that of its main cells (corneocytes), on early indications of skin damage should be investigated with a focus. Indeed, corneocytes suffer a maturation process as they move upwards in the SC, with the loss of intercellular junctions (corneodesmosomes, CDs) and the maturation of the cornified envelope (CE) [8]. Recently, the authors have characterised the changes in the properties of these cells in healthcare professionals following the

prolonged application of respirator protective equipment (RPE) [12]. The results revealed higher levels of immature CEs and desmoglein-1 (Dsg1), a cadherin-type cell-cell adhesion molecule found in stratified epithelial desmosomes, at the sites of mechanical load exposure from the respirator application (cheek) compared to a control site [12].

The current authors investigated changes in biophysical parameters of skin and the inflammatory cytokine responses in a cohort of hospitalised patients presenting with category I PUs [13, 14]. Significant spatial changes in skin barrier function were revealed (transepidermal water loss), and evident upregulation in proinflammatory biomarker IL-1α, suggesting that the tissue homeostasis was compromised. However, to date there has not been any investigation of the changes in the properties of skin cells from the sites of PUs. Therefore, the aim of the current study was to characterise the maturation and mechanical properties of corneocytes over the site of a category I PU from a sub-group of a cohort presenting such PUs from our previous study [13].

1 MATERIALS AND METHODS

1.1 Study protocol

The current investigation represents a secondary analysis from a cohort observational study conducted by Abiakam et al. in a large teaching hospital in the UK [13]. It was approved by the Health Research Authority committee (IRAS 301685) and written informed consent was obtained from patients prior to commencing the study. Corneocytes were collected from the investigation sites, i.e., PU-compromised area and a control site, located 10 cm lateral to the PU site (Figure S1a) from a sub-set of patients (n=17) from the original cohort of 30 who presented with category 1 PUs. These were located in either the sacrum (n=11) or buttocks (n=6) of the patients (Figure S2), who were either in elderly care or surgical hospital wards. From this subset of patients, about 24% of them developed later stages of PU during the data collection period (up to 2 weeks). Cells were collected via tape stripping (Sellotape, UK) (Figure S1b – first tape strip was used), by pressing the tape gently onto the skin with gloved hands and removing via peeling. Each tape strip was cut into three equal parts and used for topographical and mechanical analysis via Atomic Force Microscopy (AFM) (Figure S1d), and for assessment of CE maturation and corneodesmosomes distribution (Figure S1e and S1f).

1.2 Atomic Force Microscopy

Atomic force microscopy (AFM) imaging and nanoindentation experiments were performed in air (Nanowizard 4, JPK). Standard imaging tips (NCHV-A, Bruker AFM Probes, Inc), with a nominal spring constant of 40 N/m and resonance

frequency of 300 kHz, were used. Cell roughness was measured as root mean square height deviations (S_q) and arithmetic mean height deviations (S_a) from fitted mean planes using Gwyddion software [15], by analysing three random regions of 25 μm^2 per cell. The geometry of each AFM tip was calibrated as described in the Supplementary Information (S2). Corneocytes were extracted from the tape by pressing the tape onto a microscope glass slide by overnight incubation in xylene. Cells attached to the slide were imaged in Tapping Mode (512 x 512 pixels, 40 x 40 µm). Nanoindentation experiments consisted of 64 indents on an 8 x 8 matrix, with points spaced 625 nm apart. Five cells were evaluated per sample. Force curves consisted of loading-pause-unloading cycles, with a maximum applied force of 1–2 µN. When this force setpoint was reached during loading, the cell was allowed to relax for a period of 4 s at a constant height. After this period, the AFM probe was retracted from the surface. The Young's modulus of corneocytes was calculated using the Oliver-Pharr analysis, as described in the Supplementary Information (S3).

CE maturity assay: CE extraction and immunostaining for involucrin and Nile red staining for lipids

Cornified envelopes were isolated from the tape using an established methodology [16] and processed using a standardised protocol [12]. In summary, half of each tape was extracted with 750 mL of dissociation buffer containing 100 mM Tris-HCl pH 8.0, 5 mM EDTA (ethylenediaminetetraacetic acid), 2% SDS (sodium dodecyl sulphate) and 20 mM DL-dithiothreitol (Sigma Aldrich Dorset,

UK). The tapes were extracted in the dissociation buffer for 10 min at 75 °C and centrifuged at room temperature for 10 min at 5000 g. The extracted CEs were washed three times and suspended in 1 × PBS buffer (Sigma Aldrich Dorset, UK). Extracted CEs were transferred onto a Polysine-coated microscope slide (5 µL, VWR International Ltd, Leicestershire, UK) and incubated overnight in a humidity chamber at 4°C with a primary monoclonal antibody against involucrin (1:100, mouse anti-human involucrin SY5, ABCAM, Cambridge, UK). The antibody solution was washed with PBS three times for 5 min before adding the secondary antibody Alexa-Fluor 488-labeled goat anti-mouse IgG antibody (1:200, ABCAM, Cambridge, UK) for 60 min at room temperature (in the dark). The slides were washed with 1 × PBS (three times for 5 min) and a cover slip was mounted with 20 µg/mL Nile red (Sigma Aldrich, Dorset, UK) in 75% glycerol solution (w/w).

Immunostaining for Dsg1

The prevalence of corneodesmosomes was indirectly measured by immunostaining of desmoglein-1 (Dsg1). The immunostaining protocol for Dsg1 was adapted from a previous study [12]. Here, corneocytes were extracted from the tape onto a glass slide via overnight immersion in xylene to avoid residual fluorescent background from the tape (Figure S1c). Attached cells were washed with 1 × PBS (10 min) and incubated with a P23 mouse monoclonal antibody against the extracellular domain of Dsg1 (Progen, Heidelberg, Germany) at 4 °C overnight. This was followed by incubation with Alexa-Fluor 488-labeled goat

anti-mouse IgG antibody (1:200, ABCAM, Cambridge, UK), for 60 min at room temperature in the dark. The samples were mounted with anti-fade fluorescence mounting medium (ABCAM, Cambridge, UK).

Image analysis

Optical image analysis was performed as previously described [12]. Briefly, five non-overlapping images were taken in total for each CE and Dsg1 sample at a 10× objective magnification and analysed using a Leica DMRBE microscope (Leica Microsystems, USA) equipped with PL-Fluotar 5×/0.12 and 10×/0.30 lenses mounted with a Cool-LED pE-300 series blue-illumination source at the wavelength of 460 nm and with a Motic Pro 252 microscope camera. Images were analysed using ImageJ® version 1.53a (National Institutes of Health, Bethesda, MD, USA).

CE maturation was evaluated using a sequential approach [12]. Images were converted to either an 8-bit map (for total cell number count) or divided in RGB channels (to count cells staining for Alexa-Fluor 488, i.e., positive to involucrin). The Huang threshold followed by the Watershed command was applied to define CE borders and the cells with a surface area of 300-2000 μm^2 were counted. For the distribution of Dsg1, the ratio of pixels expressing Dsg1 to the total area in pixels was counted in two random regions of interest (ROIs) of 70 x 70 µm containing corneocytes.

1.3 Statistical analysis

Raw data were imported into IBM® SPSS® Statistics (version 27) for analysis and assessed for normality using probability plots and the Shapiro-Wilk test for each site, which revealed a normal distribution for morphological and maturation properties (% INV+ and Dsg1) and a non-normal distribution for the Young's modulus. Accordingly, a t-student or Mann-Whitney test was employed to investigate whether the anatomical sites presented differences in morphological and maturation properties, and moduli values, respectively. Tests were considered statistically significant at a 5% level ($p < 0.05$).

RESULTS

A cohort of 17 patients (13 males and 4 females) presenting with category 1 PUs were recruited for the study. Patients were of a white ethnic background and ages ranging between 71 and 95 years (mean age = 86.4 ± 6.7 years) with a mean height and weight of 1.69 ± 0.08 m and 66.0 ± 17.7 kg, respectively. 41% were bedridden and 59% needed assistance with mobility. Moreover, 24% of the patients presented a history of PUs and 59% were incontinent for urine or faeces, or both.

1.4 Corneocytes at PU site presented altered topography and size compared to the control site

Representative topographical images obtained using TM AFM of superficial corneocytes collected at a site of category1 PU and a control site (10 cm adjacent to PU site) from six of the 17 patients are presented in Figure 1. All images for the patient cohort can be found in the Supplementary Information (Fig. S5). At the control site, corneocytes were characterised by ridges and valleys, with average roughness values (Table 1). However, some patients presented circular nano-objects (CNOs) at the cell surface (Figure S5 – P8, P11, P17). Patient 9 presented deformed topography without visible recognisable features (Figure 1).

By contrast, at the PU site, most patients exhibited visible changes in topography, frequently presenting CNOs (Figure 1 – P2, P5, P10, P17, Figure S5 – P2, P3, P5, P6, P8, P10, P11, P12, P14, P16, P17), or deformed topography (Figure 1 – P9, P16). These differences between the PU and control sites were

quantified as an increase in S_q roughness values (Table 1, Figure S4), with averages of 84.1 ± 18.1 nm at the PU site compared to the control site of 55.4 ± 18.5 nm ($p<0.001$).

The size of corneocytes were measured using AFM and the size of isolated CEs from double staining against INV+ and with Nile red (Table 1). Corneocytes were smaller at the PU site compared to the control site, although a statistically significant difference was only found for isolated CEs ($p<0.05$).

1.5 Levels of immature CEs were elevated at category 1 PU site

The level of immature CEs was studied at the PU and control sites, as the ratio between INV+ CEs and the total number of CEs. The results are shown in Figure 2 for the patients showing the greatest changes between the two sites. Representative microscopy images for all patients can be found in the Supplementary Information (Figure S6).

Most patients, except P1, P3 and P4, had higher levels of immature CEs at the PU site compared to the control site (Figure 2, 3a and S6). There was a significant difference (Figure 3b, $p<0.001$) in levels of immature CEs between the PU (mean ± standard deviation = 44.7 ± 12.1%) and control site (mean ± standard deviation = 26.9 ± 10.1%) within the cohort.

1.6 Levels of Dsg1 were elevated at category 1 PU site

Representative images from the immunostaining of Dsg1 are shown in Figure 4 for the patients showing the largest changes between the two sites of investigation, with the entire image data set for the 17 patients provided in the Supplementary Information (Figure S7).

A honeycomb pattern of Dsg1 was prevalent for control site samples, except for participant P9 and P12 whose samples had a uniform distribution of Dsg1 signal over the cell surface. In contrast, at the PU sites, Dsg1 was present not just at the cell periphery, but also in the central regions of the cells for all patients except P7, P12 and P14. Individual data are shown in Figure 3c and show greater levels of Dsg1 for 12 out of 17 participants (namely P2, P3, P4, P6, P7, P8, P10, P11, P13, P15, P16 and P17). Indeed, the average Dsg1 value for the PU site samples was 43.7 ± 14.6%, which was significantly higher (Figure 3d, $p<0.001$) than for control site samples (25.8 ± 10.6%).

1.7

1.8 Corneocytes at category 1 PU sites present similar stiffness values to the control site

The Young's modulus of the corneocytes was measured using AFM and the results are presented in Figure 5. There were no significant differences in the cell stiffnesses between the two sites (Figure 5b). However, there was a high degree of inter-subject variability (Figure 5a), with coefficients of variation of 43% and 46% for the control and PU sites, respectively. For example, at the PU site, while patients P2, P12, P13, P14 and P15 had relatively larger values of the modulus (medians were 514, 530, 435, 586 and 598 MPa, respectively), other patients,

such as P3, P9, P10, P11 and P17 had lower moduli values (medians were 175, 195, 193, 152 and 140 MPa, respectively).

DISCUSSION

The mechanisms underlying the superficial changes in skin over a PU site are still not fully understood and the role of the SC in both loss of tissue integrity and recovery have been mostly neglected. In this context, the aim of the present study was to investigate the properties of corneocytes collected from a category 1 PU and an adjacent control site. The maturation, topography, area and stiffness of corneocytes were analysed to characterise local changes in cell properties. The results revealed altered topography of PU corneocytes, characterised by the presence of CNOs, which was reflected in increased cell roughness values. Moreover, changes in the maturation properties of cells at the PU sites were observed, with increased levels of immature CEs and Dsg1. These differences could correspond to local changes in the skin barrier function and be a potential marker for diagnosing early signs of damage.

There was a trend for the average size of the corneocytes via AFM topography to be greater than those obtained by fluorescence microscopy of extracted CEs (Table 1). This may be due to the multi-step process used to extract CEs from the tape and separating them individually. Although the level of structural changes provoked by the extraction protocol was not studied, some changes to the keratin matrix are expected due to the denaturing nature of some materials (e.g., SDS), which may render a less rigid form. Nonetheless, both methods resulted in similar size trends, i.e., corneocytes at PU sites were generally smaller than those at the control site. The lack of a statistical significance in the case of AFM data may be due to the number of cells analysed,

which were five per subject and body site, whereas 10 times more CEs were analysed per subject and body site.

The topographical analysis of superficial corneocytes revealed changes in the surface features and morphology of cells in category 1 PUs (Figure 1 and Table 1). Cells at the control site were generally smooth (Table 1), characterised by cross-over ridges and valleys (Figure 1). By contrast, PU corneocytes were rough ($p<0.001$), presenting CNOs over the cell surface. Two patients, P9 and P16, displayed a distorted cell surface with little or no distinct topographical features (Figure 1). CNOs have been previously detected for certain skin conditions [17-20], such as Atopic Dermatitis [18]. They have also been associated with the exposure of chemicals on the skin such as sodium dodecyl sulphate [20]. In those studies, the presence of such structures was related to changes in the skin barrier function (TEWL) [18, 20]. Indeed, in our previous published study, a significant increase in TEWL was registered at the PU sites, while control sites 5 and 10 cm away generally conformed to normative values [13].

Furthermore, CNOs have been previously shown to harbour corneodesmosin, a glycoprotein located in the core of corneodesmosomes [18, 21]. These structures were suggested to likely be involved in cell-to-cell attachment [17]. Interestingly, in addition to the increase in CNOs, an increase in the levels of Dsg1 (a component of corneodesmosomes) was also found at the PU sites compared to the control sites (Figure 3c, 3d and 4). This non-peripheral distribution (homogenous pattern) of Dsg1 has been suggested to lead to

cracking of the SC with the formation of hexagonal scaling clinical features when the skin is subjected to lateral-pulling forces [22]. The consequences of increased levels of Dsg1 in PU corneocytes should be further investigated, since an increase in SC cohesion (cells strongly attached to each other) may influence skin resistance to pressure and shear forces.

Moreover, the current study has revealed an increase in the level of immature CEs at the PU sites ($p<0.001$). Increased levels of immature CEs have been previously observed in irritated skin [23] and scaly inflammatory dermatoses [24, 25] and related to impaired barrier function [23]. The formation of a mature CE is a complex process regulated by factors such as a calcium gradient and certain cytokines. These signalling molecules control the expression of structurally important proteins involved in building the CE (interleukin-31), as well as in the lipid composition of the CE (interferon-γ) and in cell-to-cell adhesion (interleukin-1α, IL-1α) [25]. A complimentary analysis of the category 1 PU patients in the present study revealed an upregulation of IL-1α, compared to a negative control site [14]. Therefore, the increased level of immature CEs found in this study may be due a cytokine action on certain signalling pathways, namely the release of pro-inflammatory proteins.

The study of corneocyte stiffness revealed considerable inter-subject variability, with the Young's moduli ranging from 60 to 640 MPa at the control site, and 140 to 600 MPa at the PU site (Figure 5a), but without significant differences between the PU and control sites since the median values at both sites $\approx$ 310 MPa (Figure 5b). Previous studies of isolated SC have observed an increase in

the values of the Young's modulus of SC with age [26, 27]. In fact, CEs from aged skin have been observed to present a reduced amount of loricrin and filaggrin, and an increase in small proline-rich proteins [28]. Moreover, the reduced levels of filaggrin may compromise the keratin assembly and cross-linking. Further research should analyse the modulus of corneocytes from elderly healthy subjects, enabling comparisons with hospitalized individuals. This would establish maturation and mechanical property thresholds for healthy and compromised skin.

The current study is limited by the relatively small sample size (17 patients) and a homogeneous cohort of elderly Caucasian individuals, which limits the generalisability of the results to other age groups and ethnic backgrounds. Furthermore, corneocytes were collected from a control site away from the PU site, but there was no control for elderly healthy subjects. Previous studies have shown that cells from aged skin are usually thinner and larger in area [29], but with no alteration of the number of CNOs [30]. Moreover, due to ethical constraints of the study, biopsies were not taken from the skin of deeper layers, preventing histological evaluations. This is something to consider in future studies in order to corroborate changes in deeper layers of the SC and epidermis.

Detecting early skin damage is vital for effective preventive strategies. However, even experienced clinicians face the challenges of a subjective evaluation by visual observations to detect PUs [31, 32]. Prior theories overlooked SC's role in tissue integrity. This research finds early skin damage affects corneocytes, prompting investigation into underlying pathways.

Determining if they stem from inflammation or microclimate/mechanical forces that remove the outermost cell layers could provide deeper insights into PU causes.

In summary, the present study revealed distinct changes in the topographical, maturation and CE area properties of superficial corneocytes in category 1 PUs when compared to a healthy adjacent site. Topographic features in the PU sites included the presence of CNOs, as well as increased levels of Dsg1 in the central surface regions of the cells. Moreover, an increase in the levels of immature CEs was observed, in the absence of mechanical stiffness differences. Thus, this study demonstrates that early skin damage can be characterised by changes in superficial skin cells, which are active components of the first skin barrier i.e., the SC. Future research should focus on the changes of elderly skin cells compared to those from young skin, and different skin damage mechanisms e.g., moisture, biochemical and mechanical, to understand the role of the SC in maintaining skin tissue integrity.

DATA AVAILABILITY

The data that support the findings of this study are available from the corresponding author upon request.

CONFLICT OF INTEREST

The authors have no conflicts of interest.

ACKNOWLEDGEMENTS

The authors wish to thank all the patients and the healthcare professionals who engaged with the study for their commitment.

This work was supported by the European Union's Horizon 2020 research and innovation programme under the Marie Skłodowska-Curie grant agreement No. 811965 (Project STINTS - Skin Tissue Integrity under Shear).

REFERENCES

[1] C. Bouten, C. Oomens, D. Colin, D. Bader, The Aetiopathology of Pressure Ulcers: A Hierarchical Approach, in: D.L. Bader, C.V.C. Bouten, D. Colin, C.W.J. Oomens (Eds.), Pressure Ulcer Research: Current and Future Perspectives, Springer, Berlin, Heidelberg, 2005, pp. 1-9.

[2] A. Gefen, D.M. Brienza, J. Cuddigan, E. Haesler, J. Kottner, Our contemporary understanding of the aetiology of pressure ulcers/pressure injuries, Int. Wound J. 19(3) (2022) 692-704.

[3] D.R. Berlowitz, D.M. Brienza, Are all pressure ulcers the result of deep tissue injury? A review of the literature, Ostomy Wound Management 53(10) (2007) 34-8.

[4] M.A. Ankrom, R.G. Bennett, S. Sprigle, D. Langemo, J.M. Black, D.R. Berlowitz, C.H. Lyder, Pressure-related deep tissue injury under intact skin and the current pressure ulcer staging systems, Adv. Skin Wound Care 18(1) (2005) 35-42.

[5] D.L. Bader, The last hurrah, J. Tissue Viability 31(3) (2022) 373.

[6] J.W.Y. Jor, M.D. Parker, A.J. Taberner, M.P. Nash, P.M.F. Nielsen, Computational and experimental characterisation of skin mechanics: identifying current challenges and future directions, Wiley Interdiscip. Rev. Syst. Biol. Med. 5(5) (2013) 539-556.

[7] B. Lynch, H. Pageon, H. Le Blay, S. Brizion, P. Bastien, T. Bornschlögl, et al., A mechanistic view on the aging human skin through ex vivo layer-by-layer analysis of mechanics and microstructure of facial and mammary dermis, Sci. Rep. 12(1) (2022) 849.

[8] A.S. Évora, M.J. Adams, S.A. Johnson, Z. Zhang, Corneocytes: relationship between structural and biomechanical properties, Skin Pharmacol. Physiol. 34(3) (2021) 146-161.

[9] A. Park, C. Baddiel, Rheology of stratum corneum-I: A molecular interpretation of the stress-strain curve, J. Soc. Cosmet. Chem. 23(1) (1972) 3-12.

[10] I.C. Mackenzie, The Cellular Architecture of the Stratum Corneum, in: R. Marks, G. Plewig (Eds.) Stratum Corneum, Springer, Berlin, Heidelberg, 1983, pp. 146-152.

[11] A. Kalra, A. Lowe, A.A. Jumaily, An overview of factors affecting the skins Young's modulus, J. Aging Sci. 4 (2016) 1-5.

[12] A.S. Évora, N. Abiakam, H. Jayabal, P.R. Worsley, Z. Zhang, S.A. Johnson, et al., Characterisation of superficial corneocytes in skin areas of the face exposed to prolonged usage of respirators by healthcare professionals during COVID-19 pandemic, J. Tissue Viability 32(2) (2023) 305-313.

[13] N.S. Abiakam, H. Jayabal, D. Filingeri, D.L. Bader, P.R. Worsley, Spatial and temporal changes in biophysical skin parameters over a category I pressure ulcer, Int. Wound J. (2023) 1-13.

[14] H. Jayabal, N.S. Abiakam, D. Filingeri, D.L. Bader, P.R. Worsley, Inflammatory biomarkers in sebum for identifying skin damage in patients with a Stage I pressure ulcer in the pelvic region: A single centre observational, longitudinal cohort study with elderly patients, Int. Wound J. (2023) 1-14.

[15] J.E. Sader, R. Borgani, C.T. Gibson, D.B. Haviland, M.J. Higgins, J.I. Kilpatrick, et l., A virtual instrument to standardise the calibration of atomic force microscope cantilevers, Rev. Sci. Instrum. 87(9) (2016) 093711.

[16] D. Guneri, R. Voegeli, S.J. Gurgul, M.R. Munday, M.E. Lane, A.V. Rawlings, A new approach to assess the effect of photodamage on corneocyte envelope maturity using combined hydrophobicity and mechanical fragility assays, Int. J. Cosmet. Sci. 40 (2018) 207-216.

[17] C. Riethmüller, Assessing the skin barrier via corneocyte morphometry, Exp. Dermatol. 27(8) (2018) 923-930.

[18] C. Riethmuller, M. McAleer, S. Koppes, R. Abdayem, J. Franz, M. Haftek, et al., Filaggrin breakdown products determine corneocyte conformation in patients with atopic dermatitis, J. Allergy Clin. Immunol. 136(6) (2015) 1573-1580.e2.

[19] C. Feuillie, P. Vitry, M.A. McAleer, S. Kezic, A.D. Irvine, J.A. Geoghegan, et al., Adhesion of Staphylococcus aureus to corneocytes from atopic dermatitis patients is controlled by natural moisturizing factor levels, mBio 9(4) (2018) e01184-18.

[20] C. Vater, A. Apanovic, C. Riethmüller, B. Litschauer, M. Wolzt, C. Valenta, et al., Changes in skin barrier function after repeated exposition to phospholipid-

based surfactants and sodium dodecyl sulfate in vivo and corneocyte surface analysis by atomic force microscopy, Pharmaceutics 13(4) (2021) 436.

[21] N. Jonca, M. Guerrin, K. Hadjiolova, C. Caubet, H. Gallinaro, M. Simon, et al., Corneodesmosin, a component of epidermal corneocyte desmosomes, displays homophilic adhesive properties, J. Biol. Chem. 277(7) (2002) 5024-9.

[22] Y. Kitajima, Implications of normal and disordered remodeling dynamics of corneodesmosomes in stratum corneum, Dermatologica Sinica 33(2) (2015) 58-63.

[23] T. Hirao, M. Denda, M. Takahashi, Identification of immature cornified envelopes in the barrier-impaired epidermis by characterisation of their hydrophobicity and antigenicities of the components, Exp. Dermatol. 10(1) (2001) 35-44.

[24] T. Hirao, T. Terui, I. Takeuchi, H. Kobayashi, M. Okada, M. Takahashi, et al., Ratio of immature cornified envelopes does not correlate with parakeratosis in inflammatory skin disorders, Exp. Dermatol. 12(5) (2003) 591-601.

[25] K.H. Hänel, C. Cornelissen, B. Lüscher, J.M. Baron, Cytokines and the skin barrier, Int. J. Mol. Sci. 14(4) (2013) 6720-6745.

[26] K. Biniek, J. Kaczvinsky, P. Matts, R.H. Dauskardt, Understanding age-induced alterations to the biomechanical barrier function of human stratum corneum, J. Dermatol. Sci. 80(2) (2015) 94-101.

[27] Y. Hara, Y. Masuda, T. Hirao, N. Yoshikawa, The relationship between the Young's modulus of the stratum corneum and age: a pilot study, Skin Res. Technol. 19(3) (2013) 339-345.

[28] M.K. Streubel, M. Rinnerthaler, J. Bischof, K. Richter, Changes in the Composition of the Cornified Envelope During Skin Aging: A Calcium Centric Point of View, in: M.A. Farage, K.W. Miller, H.I. Maibach (Eds.), Textbook of Aging Skin, Springer, Berlin, Heidelberg, 2014, pp. 1-20.

[29] A.V. Rawlings, The Stratum Corneum and Aging, in: M.A. Farage, K.W. Miller, H.I. Maibach (Eds.), Textbook of Aging Skin, Springer, Berlin, Heidelberg, 2017, pp. 67-90.

[30] J. Franz, M. Beutel, K. Gevers, A. Kramer, J. Thyssen, S. Kezic, et al., Nanoscale alterations of corneocytes indicate skin disease, Skin Res. Technol. 22(2) (2016) 174-80.

[31] D. Payne, Not just another rash: management of incontinence-associated dermatitis, Br. J. Community Nurs. 21(9) (2016) 434-440.

[32] J. Kottner, T. Dassen, Pressure ulcer risk assessment in critical care: Interrater reliability and validity studies of the Braden and Waterlow scales and subjective ratings in two intensive care units, Int. J. Nurs. Stud. 47(6) (2010) 671-677.

Table 1. Cell roughness and area. AFM cell area was obtained from larger TM AFM images of individual corneocytes while FM CE area was calculated from isolated CEs and double stained against INV+ and with Nile red. Roughness values measured from TM AFM images of corneocytes in a 20 × 20 µm area. S_q (root mean square height) and S_a (arithmetic mean height) of three 5 × 5 µm regions (n =5 cells per site per participant). Results are presented as mean ± 1 SD. FM = Fluorescence Microscopy

Parameter	Control Site	PU site	p-value
S_q (nm)	55.4 ± 18.5	84.1 ± 18.1	<0.001
S_a (nm)	44.3 ± 14.9	67.6 ± 14.8	<0.001
AFM Cell Area (nm^2)	963.7 ± 149.4	884.9 ± 188.0	ns
FM CE Area (nm^2)	667.5 ± 110.7	593.8 ± 90.4	<0.05

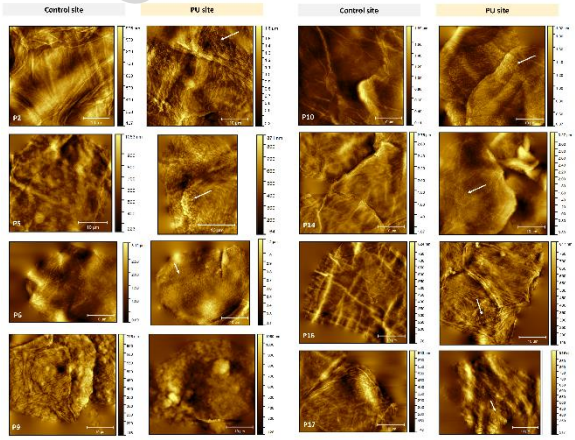

Figure 1. AFM analysis of superficial corneocytes revealed differences in the topography at the sites of the category 1 PUs. At the control sites, cells showed typical features of ridges, valleys, and peaks, with only a few patients presenting altered cell topography (e.g., P6 and P17). Cells at the PU sites exhibited an abundance of CNOs indicated by white arrows (e.g., P5, P6, P10) or a deformed topography (P9). The results for 8 patients are shown, but representative images for all 17 patients can be found in Supplementary Information. Surface height profiles and 3D plots for P10 can be found in Fig. S4.

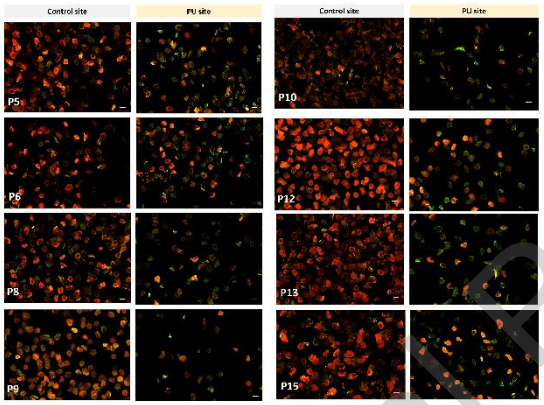

Figure 2. PU corneocytes presented high levels of immature CEs. Imaging of the control and PU sites of the superficial CEs using a double staining: immunostaining against INV (green) and Nile red (red) against lipids to quantify the degree of CE maturation for patients 5, 6, 8, 9, 10, 12, 13 and 15. The control site corneocytes stained strongly with Nile red, while the PU corneocytes presented less lipids at the surface as observed by staining green to INV. Scale bar = 50 µm.

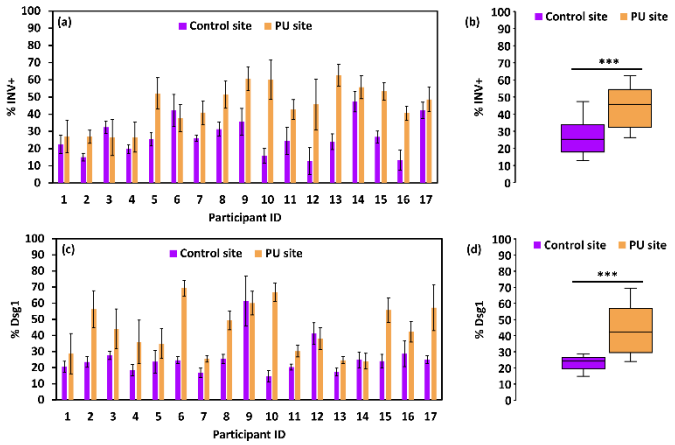

Figure 3. Individual data for the levels of immature CEs and Dsg1. (a) Individual level of % INV CEs and **(c)** % Dsg1 associated with the 17 patients. The cohort results are shown in plots **(b)** and **(d)** for % INV+ and % Dsg1, respectively as box-and-whisker plots. The box boundaries indicate the 25th and 75th percentiles, while the whiskers represent the 10th and 90th percentile. The median is represented by the line (—). Independent sample t-tests were performed. ***p<0.001

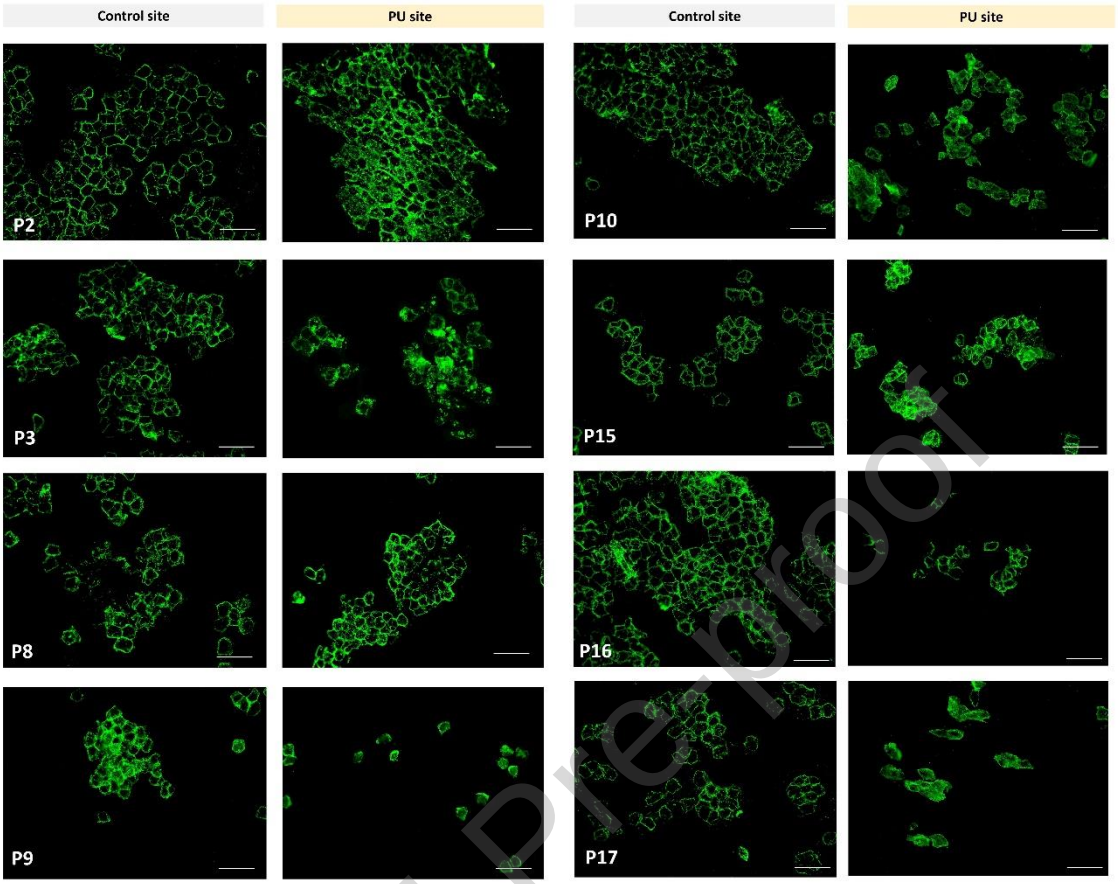

Figure 4. PU samples presented higher levels of Dsg1 staining. Distribution of Dsg1 at the surface of superficial corneocytes as an indirect measure of CDs. Most patients had a typical honeycomb pattern with Dsg1 mostly at the cell periphery of the control site. However, the corneocytes at the PU sites showed varying degrees of a more uniform distribution of Dsg1 over the cell surface across the cohort. Scale bar = 100 µm.

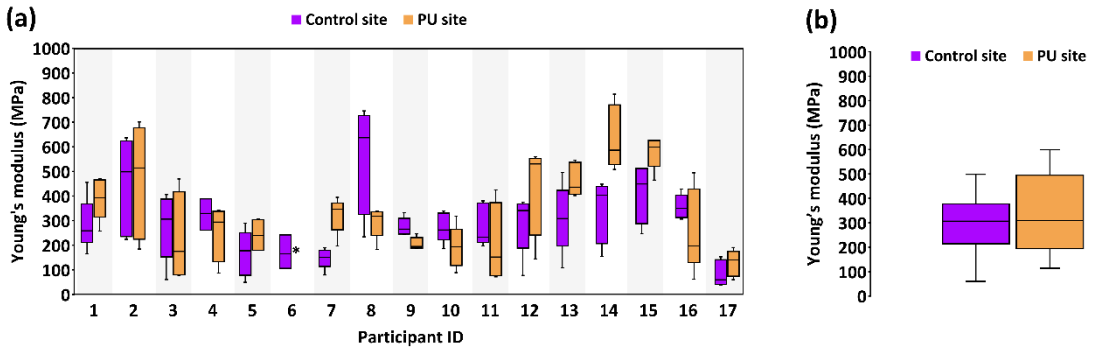

Figure 5. Box-and-whisker plots of individual cell stiffness data. (a) Young's modulus and **(b**) cohort results. The upper and lower whiskers represent the highest and lowest datum within 1.0 interquartile range. (n = 5 cells per site per participant) *indicates missing data

Credit author statement

Ana S. Évora: Conceptualization; Data curation; Formal analysis; Investigation; Methodology; Writing - original draft.

Nkemjika Abiakam: Conceptualization; Investigation; Methodology.

Zhibing Zhang: Supervision; Writing - review & editing.

Simon A. Jonson: Project administration; Methodology; Writing - review & editing.

Michael J. Adams: Funding acquisition; Project administration; Supervision; Methodology; Writing - review & editing.

Dan L. Bader: Conceptualization; Funding acquisition.

Peter R. Worsley: Conceptualization; Supervision; Writing - review & editing.

Highlight

- This is the first cohort study that has investigated the changes in the properties of corneocyte over category I PUs.
- Superficial cells at the PU sites showed altered topographical and maturation characteristics.

- Topographic features in the PU sites included the presence of circular nano-objects, as well as increased levels of desmoglein-1 in the central surface regions of the cells and an increase in the levels of immature cornified envelopes.